PROCEEDINGS OF SCIENCE

Muon decay with light boson emission in muonic atoms

Yuichi Uesaka*
Physics Department, Saitama University, 255 Shimo-Okubo, Sakura-ku, Saitama, Saitama 338-8570, Japan
E-mail: uesaka@krishna.th.phy.saitama-u.ac.jp

There are many motivations for introducing new extra bosons to extend the standard model of particle physics. If there exists a boson X which is lighter than muon and neutral, the rare decay of muon, $\mu \to eX$, could happen.
In this article, we investigate the $\mu^- \to e^- X$ process in muonic atoms. By calculating the spectrum of the emitted electron for several cases, the model-discriminating power is discussed. We report the characteristic model-dependence of the spectrum near the endpoint, which implies that the future experiments using muonic atoms would be good probes for unknown invisible bosons.

The 21st international workshop on neutrinos from accelerators (NuFact2019)
August 26 - August 31, 2019
Daegu, Korea

*Speaker.

PoS(NuFact2019)086

1. Introduction

The standard model (SM) of particle physics is known to be insufficient to explain all phenomena, so it should be extended to introduce dark matters, neutrino masses, and so on. Although there are many possibilities to extend the SM, the clue might be hidden in low energy scale. Indeed, some phenomenological models beyond the SM introduce new neutral bosons with mass of MeV or less: e.g. the majoron, familon, or axion-like particle, or extra gauge boson.

Assuming that there exists a neutral boson X whose mass is lighter than a muon, the exotic muon decay $\mu \to eX$ could be induced [1]. By Judidio *et al.*, the decay mode $\mu^+ \to e^+\gamma$ was searched by using the highly polarized beam of positive muons, and the stringent constraint for the branching ratio was given as $Br(\mu^+ \to e^+X) < 2.6 \times 10^{-6}$ for massless X [2]. After Ref. [2], the TWIST collaboration investigated the $\mu^+ \to e^+X$ process more carefully for the wide mass region of the boson X and the various possibility of the angular distribution of the emitted electron [3]. In the future, new searches are planned at the Paul Scherrer Institute (PSI) for the region of 25MeV$<$ $m_X < 95$MeV [4], where m_X is the mass of a new boson X. Here, the explorable region of m_X has a lower limit due to the steep edge of the electron spectrum from the dominant background process, $\mu^+ \to e^+\nu_e\overline{\nu}_\mu$. That is, the further updates of the constraint for small m_X would be challenging in future experiments using positive muons.

In 2011, the use of muonic atoms was proposed to investigate the $\mu \to eX$ process [5]. In contrast to free positive muons, it could evade the contamination from the steep edge of the background spectrum for the tiny m_X. According to Ref. [5], the COMET and Mu2e experiments could be able to search for $\mu^- \to e^-X$ with the comparable sensitivity as the current constraints from the searches using free positive muons.

The aim of this work is to clarify the model-dependence of the electron spectrum in the $\mu^- \to e^-X$ process in muonic atoms. In Section 2, we show the formulation for the spectrum, taking into account various possibilities for the properties of the boson X. The numerical results are shown and the model-dependence is discussed in Section 3. Finally, we summarize this article in Section 4.

2. Formulation

In this article, we consider the following three simple effective models:

1. X is a scalar field and the effective interaction to charged leptons is

$$\mathscr{L}_{S_0} = X\overline{e}\left(g_L^{S_0}P_L + g_R^{S_0}P_R\right)\mu + [H.c.], \tag{2.1}$$

   where $P_{L/R} = (1 \mp \gamma_5)/2$ and $g_{L/R}^{S_0}$ are dimensionless coupling constants. This case was also assumed in Ref. [5].

2. X is a scalar field and the effective interaction to charged leptons is

$$\mathscr{L}_{S_1} = (-i)\frac{\partial^\alpha X}{\Lambda}\overline{e}\gamma_\alpha\left(g_L^{S_1}P_L + g_R^{S_1}P_R\right)\mu + [H.c.], \tag{2.2}$$

where Λ is an arbitrary scale to keep coupling constants $g_{L/R}^{S_1}$ dimensionless. If both a muon and an electron are in free space, the Dirac equation ensures that the interaction (2.2) is essentially equivalent to the previous interaction (2.1). However, the two could make difference for processes in a nuclear Coulomb potential.

3. X is a vector field and the effective interaction to charged leptons is

$$\mathscr{L}_{V_1} = \frac{X^{\alpha\beta}}{\Lambda}\bar{e}\sigma_{\alpha\beta}\left(g_L^{V_1}P_L + g_R^{V_1}P_R\right)\mu + [H.c.], \tag{2.3}$$

where $X^{\alpha\beta} = \partial^\alpha X^\beta - \partial^\beta X^\alpha$ is the field strength of the X field. The couplings $g_{L/R}^{V_1}$ are also dimensionless.

In a standard manner, the decay rate of $\mu^- \to e^- X$ in a muonic atom can be written as

$$\Gamma = \left(\sum_{s_e}\int \frac{d^3p_e}{(2\pi)^3 2E_e}\frac{d^3p_X}{(2\pi)^3 2E_X}\right)\left(\frac{1}{2}\sum_{s_\mu}\right)|\mathscr{M}|^2(2\pi)\delta\left(E_e + E_X - m_\mu^*\right). \tag{2.4}$$

Here $m_\mu^* = m_\mu - B_{\mu N}^{1s}$, where $B_{\mu N}^{1s}$ is the binding energy between the nucleus and muon in a $1s$ state. s_ℓ ($\ell = \mu, e$) indicates the spin of the lepton ℓ, and the factor of $1/2$ comes from the spin average of the bound muon. The amplitude $\mathscr{M}$ consists of the overlap integrals among the wave functions of muon, electron, and boson X. The nucleus is treated as an infinitely heavy object in this stage, but we will consider the finite nuclear mass approximately in the last paragraph of this section.

After straightforward calculation, we obtain the explicit formulas. For simplicity, we neglect the electron mass m_e in the following expressions, which has little effect on numerical results. The boson X is also assumed to be massless hereafter because the use of muonic atoms would be more important for smaller-mass region.

The spectrum for the first model, Eq. (2.1), is given as

$$\frac{d\Gamma}{dE_e} = \frac{\left|g_L^{S_0}\right|^2 + \left|g_R^{S_0}\right|^2}{8\pi^2} p_e p_X \sum_\kappa (2j_\kappa + 1)\left|I_{gG}^{\kappa,(0)} - I_{fF}^{\kappa,(0)}\right|^2. \tag{2.5}$$

The overlap integrals are defined as

$$I_{hH}^{\kappa,(d)} = \int_0^\infty dr r^2 j_{l_\kappa + d}(p_X r)\, h_{E_e}^\kappa(r) H(r), \tag{2.6}$$

where $j_l(r)$ is the l-order spherical Bessel function. Here, $h = g, f$ ($H = G, F$) is the radial wave function of the scattering electron (the bound muon). The index κ represents the angular momentum of the electron [6, 7]. This analytic result is consistent with that in Ref. [5].

The similar expression for the spectrum can be obtained for the remaining cases. For the second model, Eq. (2.2),

$$\frac{d\Gamma}{dE_e} = \frac{\left|g_L^{S_1}\right|^2 + \left|g_R^{S_1}\right|^2}{8\pi^2}\frac{p_e p_X^3}{\Lambda^2}\sum_\kappa (2j_\kappa + 1)\left|S_\kappa\right|^2, \tag{2.7}$$

where

$$S_\kappa = I_{gG}^{\kappa,(0)} + I_{fF}^{\kappa,(0)} + \frac{\kappa - l_\kappa}{2l_\kappa+1} I_{fG}^{\kappa,(+1)} + \frac{2+\kappa+l_\kappa}{2l_\kappa+1} I_{gF}^{\kappa,(+1)} + \frac{1+\kappa+l_\kappa}{2l_\kappa+1} I_{fG}^{\kappa,(-1)} + \frac{1+\kappa-l_\kappa}{2l_\kappa+1} I_{gF}^{\kappa,(-1)}. \tag{2.8}$$

For the third model, Eq. (2.3),

$$\frac{d\Gamma}{dE_e} = \frac{\left|g_L^{V_1}\right|^2 + \left|g_R^{V_1}\right|^2}{\pi^2} \frac{p_e p_X^3}{\Lambda^2} \sum_\kappa (2j_\kappa+1) \frac{|V_\kappa|^2}{l_\kappa(l_\kappa+1)}, \tag{2.9}$$

where

$$\begin{aligned} V_\kappa = (1+\kappa)\left(I_{gG}^{\kappa,(0)} + I_{fF}^{\kappa,(0)}\right) - \frac{l_\kappa(\kappa-l_\kappa)}{2l_\kappa+1} I_{fG}^{\kappa,(+1)} + \frac{l_\kappa(2+\kappa+l_\kappa)}{2l_\kappa+1} I_{gF}^{\kappa,(+1)} \\ + \frac{(l_\kappa+1)(1+\kappa+l_\kappa)}{2l_\kappa+1} I_{fG}^{\kappa,(-1)} - \frac{(l_\kappa+1)(1+\kappa-l_\kappa)}{2l_\kappa+1} I_{gF}^{\kappa,(-1)}. \end{aligned} \tag{2.10}$$

The nuclear mass m_N is treated infinite in Eq. (2.4). For the light nucleus, however, we should take into account a nuclear recoil in calculation for the spectrum near the endpoint. We use the well-known prescription to include the recoil effect in the final state [5, 8]:

$$E_X = m_\mu^* - E_e - \frac{E_e^2}{2m_N}. \tag{2.11}$$

Also, in the calculation of the muon wave function and binding energy, the leading correction from the finite nuclear mass is included by using the reduced mass $m_{\mu N} = m_\mu m_N/(m_N+m_\mu)$ in the Dirac equation, instead of the original muon mass m_μ [9].

3. Numerical Results

In this article, we assume the ^{27}Al target with $m_N = 25133$MeV, which will be used in the coming experiments, COMET and Mu2e. By solving the radial Dirac equation for the bound muon, we obtain the endpoint energy $E_{\rm end} = m_\mu^* - m_\mu^{*2}/2m_N = 104.98$MeV.

The numerical results for the spectrum of emitted electron is shown in Fig. 1. Seen in (a) of Fig. 1, the spectra for all models we considered have a peak around $E_e = m_\mu/2$ and the model-dependence is small. On the other hand, in the spectrum near the endpoint shown in (b) of Fig. 1, the differences between the property of the boson X are clearly seen. Since suppression near the endpoint of the spectrum for the third model is weaker than the other two models with a scalar X, $\mu^- \to e^- X$ searches using muonic atoms could be slightly more sensitive to the vector X with the dipole interaction, Eq. (2.3).

In the spectrum for the first model, there is a suppressed region near the endpoint, which is clearly seen in (c) of Fig. 1, with a logarithmic scale. The nontrivial shape can be understood by the analytic formula of the spectrum, Eq. (2.5), as follows: Although the dominant contribution in Eq. (2.5) comes from $\kappa = -1$, it vanishes at $E_e = E_{\mu N}$ due to the fact that

$$\int_0^\infty dr r^2 g_{E_e}^{-1}(r) G(r) = \int_0^\infty dr r^2 f_{E_e}^{-1}(r) F(r), \tag{3.1}$$

when the energy of the electron is the same as that of the muon [8]. For the ^{27}Al target, $E_{\mu N} = 104.75$MeV is about 200keV smaller than $E_{\rm end}$. Careful measurement of the electron spectrum near the endpoint with sufficient energy resolution would help to identify the boson X.

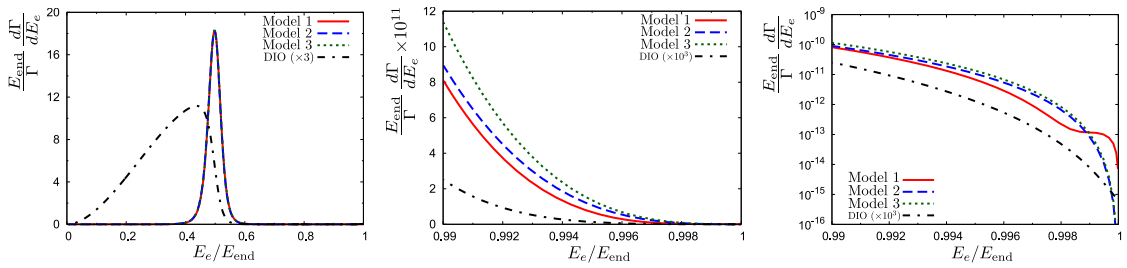

(a) (b) (c)

Figure 1: The spectrum of the emitted electron in the $\mu^- \to e^- X$ process in a muonic atom for the ^{27}Al target. The x-axis indicates the electron energy normalized by the endpoint energy $E_{\rm end}$. The y-axis indicates the spectrum $d\Gamma/dE_e$ times $E_{\rm end}$ divided by the total decay rate Γ. The solid (red), the dashed (blue), and the dotted (green) curves correspond to the models 1-3, respectively. (a) shows the region that $0 < E_e/E_{\rm end} < 1$, while (b) and (c) show the region that $0.99 < E_e/E_{\rm end} < 1$. In (c), a logarithmic scale is used on y-axis. Also, the spectrum of the decay-in-orbit (DIO) process, $\mu^- \to e^- \nu_\mu \overline{\nu}_e$, is shown by the dash-dotted (black) curve in each figure. We note that the DIO spectrum is normalized by the total DIO rate, and multiplied by factors of 3 in (a) and 10^3 in (b) and (c), for readability purposes.

4. Summary

We have investigated the $\mu^- \to e^- X$ process in muonic atoms, which is proposed in Ref. [5] as an interesting candidate to constraint the property of light neutral bosons. In this article, three simple effective models have been considered on property of the unknown boson X to reveal the model-dependence of the spectrum of the emitted electron in the $\mu^- \to e^- X$ process. As result, it is found that the spectrum near the endpoint strongly depends on the property of the boson X. Careful measurement for the electron spectrum in the muon decay should be useful to identify the property of unknown invisible bosons. We need further researches for realistic estimation of the sensitivity in future experiments.

Acknowledgments

We thank Y. Kuno, C. Wu, T. Xing, J. Sato, and T. Sato for fruitful comments. This work was supported by the Sasakawa Scientific Research Grant from the Japan Science Society.

References

[1] J. Heeck and W. Rodejohann, Phys. Lett. B **776**, 385 (2018).
[2] A. Jodidio *et al.*, Phys. Rev. D **34**, 1967 (1986).
[3] R. Bayes *et al.* (TWIST Collaboration), Phys. Rev. D **91**, 052020 (2015).
[4] A. Schöning, Talk at Flavour and Dark Matter Workshop, Heidelberg, September 28 (2017);
A. K. Perrevoort, Talk at Flavour and Dark Matter Workshop, Karlsruhe, September 26 (2018).
[5] X. G. i Tormo, D. Bryman, A. Czarnecki, and M. Dowling, Phys. Rev. D **84**, 113010 (2011).
[6] M. E. Rose, *Elementary Theory of Angular Momentum* (John Wiley & Sons, New York, 1957).
[7] M. E. Rose, *Relativistic Electron Theory* (John Wiley & Sons, New York, 1961).
[8] O. U. Shanker, Phys. Rev. D **25**, 1847 (1982).
[9] H. Grotch and D. R. Yennie, Rev. Mod. Phys. **41**, 350 (1969).